Biomarkers identification in Alzheimer's disease using effective connectivity analysis from electroencephalography recordings

Identificación de biomarcadores en la enfermedad de Alzheimer usando análisis de conectividad efectiva a partir de registros de electroencefalografía

Jazmín X. Suárez-Revelo[1], John F. Ochoa-Gómez[2], Jon E. Duque-Grajales[3], and Carlos A. Tobón-Quintero[4]

ABSTRACT

Alzheimer's disease (AD) is the most common cause of dementia, which generally affects people over 65 years old. Some genetic mutations induce early onset of AD and help to track the evolution of the symptoms and the physiological changes at different stages of the disease. In Colombia there is a large family group with the PSEN1 E280A mutation with a median age of 46,8 years old for onset of symptoms. AD has been defined as a disconnection syndrome; consequently, network approaches could help to capture different features of the disease. The aim of the current work is to identify a biomarker in AD that helps in the tracking of the neurodegenerative process. Electroencephalography (EEG) was recorded during the encoding of visual information for four groups of individuals: asymptomatic and mild cognitive impairment carriers of the PSEN1 E280A mutation, and two non-carrier control groups. For each individual, the effective connectivity was estimated using the direct Directed Transfer Function and three measurements from graph theory were extracted: input strength, output strength and total strength. A relation between the cognitive status and age of the participants with the connectivity features was calculated. For those connectivity measures in which there is a relation with the age or the clinical scale, the performance as a diagnostic feature was evaluated. We found that output strength connectivity in the right occipito-parietal region is related to age of the carrier groups ($r = -0,54$, $p = 0,0036$) and has a high sensitivity and high specificity to distinguish between carriers and non-carriers (67 % sensitivity and 80 % specificity in asymptomatic cases, and 83 % sensitivity and 67 % specificity in symptomatic cases). This relationship indicates that output strength connectivity could be related to the neurodegenerative process of the disease and could help to track the conversion from the asymptomatic stage to dementia.

Keywords: Familial Alzheimer disease, electroencephalography, effective connectivity, brain graphs.

RESUMEN

La enfermedad de Alzheimer (EA) es la causa más común de demencia, la cual afecta generalmente a personas después de los 65 años de edad. Algunas mutaciones genéticas inducen la aparición temprana de EA ayudando a monitorear la evolución de los síntomas y los cambios fisiológicos en diferentes etapas de la enfermedad. En Colombia existe un gran grupo familiar con la mutación PSEN1 E280A, con una edad media de aparición de los síntomas de 46,8 años. La EA ha sido definida como un síndrome de desconexión; en consecuencia, enfoques de redes podrían ayudar a capturar diferentes características de la enfermedad. El objetivo del presente trabajo es identificar un biomarcador en la EA que permita realizar el seguimiento del proceso neurodegenerativo. Se registró una electroencefalografía (EEG) durante la codificación de información visual en cuatro grupos de sujetos: portadores de la mutación PSEN1 E280A asintomáticos y con deterioro cognitivo leve y dos grupos control de no portadores. Para cada sujeto se estimó la conectividad efectiva utilizando la Función de Transferencia Directa dirigida y se extrajeron tres medidas de grafos: fuerza de entrada, fuerza de salida y fuerza total. Se calculó una relación entre el estado cognitivo y la edad de los participantes con las características de conectividad. Para aquellas medidas de conectividad que tuvieran una relación con la edad o la escala clínica, se evaluó su desempeño como variable de diagnóstico. Se encontró que la fuerza de conectividad saliente en la región parieto-occipital derecha está relacionada con la edad del grupo de los portadores ($r = -0,54$, $p = 0,0036$), y que tiene alta sensibilidad y especificidad para distinguir entre portadores y no portadores (67 % de sensibilidad y 80 % de especificidad en casos asintomáticos, y 83 % de sensibilidad y 67 % de especificidad en casos sintomáticos). Esta relación indica que la fuerza de conectividad saliente podría estar relacionada con el proceso neurodegenerativo de la enfermedad y podría ayudar a realizar un seguimiento de la conversión desde la etapa asintomática hacia la demencia.

Palabras clave: Enfermedad de Alzheimer familiar, electroencefalografía, conectividad efectiva, grafos cerebrales.

Introduction

Alzheimer's disease (AD) is the most prevalent cause of dementia, a neurodegenerative condition which generally affects people over 65 years old (Minati, Edginton, Bruzzone, & Giaccone, 2009). Although it is impossible to know which individuals will develop AD, some genetic mutations induce the early onset of the disease (Bertram & Tanzi, 2011) helping to follow the evolution of the symptoms and the physiological changes in early stages of the disease. In Colombia there is a large family group with the PSEN1 E280A mutation which is involved in the production of β-amyloid (Lopera *et al.*, 1997). The symptoms onset occurs at a median age of 46,8 years old (Ardila *et al.*, 2000). Given that the efficacy of some AD therapies may depend on the initiation of treatment before the onset of clinical symptoms, it is important to search for early biomarkers. Nowadays, the study of mutation carriers provides the unique opportunity to identify early changes related to predisposition to the disease (Langbaum *et al.*, 2013; Sperling, Mormino, & Johnson, 2014).

Electroencephalography (EEG) enables the investigation of early neurophysiological changes associated with neurodegenerative processes. It represents a low cost, portable and non-invasive alternative to study brain functions (Micanovic & Pal, 2014). AD has been defined as a disconnection syndrome and consequently, network approaches based on graph theory have captured different features of the disease (Bullmore & Bassett, 2011; Hafkemeijer, van der Grond, & Rombouts, 2012; He, Chen, Gong, & Evans, 2009; Ouchi & Kikuchi, 2012; Xie & He, 2011). EEG studies show that brain activity synchronization is disturbed in AD (Pievani, de Haan, Wu, Seeley, & Frisoni, 2011). Increases in delta and theta activity and decreases in coherence between brain regions have been reported (Hsiao, Wang, Yan, Chen, & Lin, 2013). Studies have shown that functional networks in AD lose their normal small-world structure, and evolve towards a more random architecture (Sanz-Arigita *et al.*, 2010; Supekar, Menon, Rubin, Musen, & Greicius, 2008). An increased vulnerability of the brain network hubs to the accumulation of β-amyloid has also been found (Stam *et al.*, 2009).

Recent studies using magnetic resonance imaging in PSEN1 E280A mutation carriers have demonstrated preclinical changes in thickness and volume across the cortex (Yakeel T Quiroz *et al., 2013)*. Changes have also been shown in regional brain activity using positron emission tomography (Fleisher *et al.*, 2015), functional magnetic resonance imaging (Yakeel T Quiroz *et al.*, 2010), spectral energy alterations in EEG, and potential modulation in event related potentials studies (Bobes *et al.*, 2010; Duque-Grajales *et al.*, 2014; Y T Quiroz *et al.*, 2011; Rodriguez *et al.*, 2014; Tobon *et al.*, 2015). These findings show the disease to be a dynamical phenomenon (Y T Quiroz *et al.*, 2011). To our knowledge, there are no studies on how the effective connectivity in the PSEN1 E280A mutation can help to differentiate pre-symptomatic and symptomatic AD PSEN1 E280A mutation carriers from non-carriers using EEG signals. We hypothesized that patients with the mutation have altered network features compared with control subjects, and this alteration could be used as a biomarker.

The aim of the current work is to identify EEG effective connectivity features that might serve as possible biomarkers in AD. Given that AD is a neurodegenerative process, the identified features should change across different years, following the pattern of neurodegeneration. Therefore, we recorded EEG during the performance of a memory encoding task for four groups of individuals: asymptomatic carriers of the PSENI E280A mutation, mutation carriers with mild cognitive impairment (MCI) and two non-carrier control groups. For each individual we evaluated the effective connectivity using the direct Directed Transfer Function (dDTF) (Delorme *et al.*, 2011). Then, we developed a statistical analysis to find a relationship between connectivity measures and age and cognitive status, and to evaluate their performance to classify subjects at risk of developing AD.

Methodology

Subjects

The subjects were members of the PSEN1 E280A mutation Colombian kindred. Fifteen asymptomatic mutation carriers (ACr) without cognitive impairment, twelve participants with MCI, and twenty-seven healthy non-carriers were matched for gender, age, and educational level with ACr group (Control1), and MCI group (Control2) (Table 1). Due to the difference in age between asymptomatic and symptomatic carriers groups, two control groups were selected. For AD the age is a critical factor and the subjects with clinical complaints are not comparable with younger subjects. Informed consent for participation was obtained from all subjects according to the protocol approved by

[1] Bioengineer, Universidad de Antioquia, Colombia. Affiliation: Grupo de investigación en Bioinstrumentación e Ingeniería Clínica (GIBIC), Universidad de Antioquia, Colombia. E-mail: jazmin.suarez@udea.edu.co

[2] Systems Engineer, Universidad Nacional, Colombia. Master in Engineering, Universidad de Antioquia, Colombia. Affiliation: Grupo de investigación en Bioinstrumentación e Ingeniería Clínica (GIBIC), Universidad de Antioquia, Colombia. E-mail: john.ochoa@udea.edu.co

[3] Bioengineer, Universidad de Antioquia, Colombia. Master in Engineering, Universidad de Antioquia, Colombia. Affiliation: Grupo de investigación en

Bioinstrumentación e Ingeniería Clínica (GIBIC), Universidad de Antioquia, Colombia. E-mail: jon.duque@udea.edu.co

[4] MD, Universidad de Antioquia, Colombia. PhD in Biomedical Basic Sciences, Universidad de Antioquia, Colombia. Grupo de Neurociencias de Antioquia (GNA), Universidad de Antioquia, Colombia. Affiliation: Grupo de Neuropsicología y Conducta, Universidad de Antioquia, Colombia. E-mail: cantobon@gmail.com

the Human Subjects Committee of the Universidad de Antioquia. In addition to the EEG records, neurological and neuropsychological tests were performed (Aguirre-Acevedo et al., 2007). All data were acquired by researchers who were blinded to the participant's genetic status. The exclusion criteria were severe physical illness, alcohol/drugs abuse, regular use of neuroleptics and antidepressants with anticholinergic action.

EEG recordings

A Neuroscan unit amplifier (Neuroscan Medical System, Neuro-soft Inc. Sterling, VA, USA) was used to record EEG signals. EEG data were recorded from 64 electrodes positioned according to the international 10-10 system with midline reference (recomputed to common average). The signal was digitized at a sampling rate of 1000 Hz and filtered online (bandpass filter: 0,05 to 200 Hz, and band reject filter 60 Hz to eliminate noise from the power supply). A simultaneous electrooculogram (0,1 ± 100 Hz bandpass) was also recorded. Recordings were obtained while subjects performed a memory encoding task using color pictures of concrete and nameable objects (Figure 1). This task is based on a paradigm previously used in the same population (Y T Quiroz et al., 2011). 50 stimuli were presented. Each trial begins with a 1000 ms fixation character ("+") prior to the presentation of the stimuli. Then, stimuli were presented for 2000 ms followed by the question, "Do you like this item?" Subjects were then prompted to press a button to signify their like/dislike judgment.

Table 1. Demographic and neuropsychological characteristics of participants.

	ACr Mean (±SD)	Control1 Mean (±SD)	Test	MCI Mean (±SD)	Control2 Mean (±SD)	Test
N	15	15	–	12	12	–
Age (years)	27,8 (±4)	31,5 (±5,8)	T = −2,04 df = 28 P = 0,05	52,9 (±10,6)	44,2 (±9,9)	T = −2,18 df = 22 P = 0,05
Gender (F/M)	9/6	9/6	$X^2 = 0$ P = 1	5/7	8/4	$X^2 = 1,51$ P = 0,22
Education (years)	12,1 (±3,3)	11,2 (±3,4)	T = 0,75 df = 28 P = 0,46	9,3 (±4,7)	9,8 (±4)	T = −0,28 df = 22 P = 0,78
MMSE	29,7 (±0,6)	29,5 (±0,9)	T = 0,22 df = 28 P = 0,83	22,2 (±4,6)	29,4 (±1,2)	T = −5,17 df = 12,37 $P = 2 \times 10^{-4}$

ACr: asymptomatic mutation carriers; MMSE: mini-mental state examination; SD: standard deviation; df: degrees of freedom; X2: chi-squared.
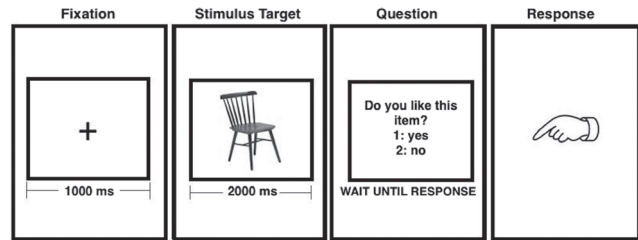

Figure 1. Scheme of memory encoding paradigm used.

Signal pre-processing

EEG data were analyzed offline for artifact correction from the implementation of an automated preprocessing pipeline using MATLAB toolbox EEGLAB (Delorme & Makeig, 2004). Data were filtered (1–50 Hz; FIR filter), bad channels were detected and interpolated using spherical splines. Then, data were segmented in epochs of 1 s, selected after stimulus presentation, and re-referenced to average. The EEG epochs with ocular, muscular, and other kinds of artifact were removed by a computerized automatic procedure based on linear trend, joint probability and kurtosis approach (Delorme, Sejnowski, & Makeig, 2007). Independent component analysis enhanced by wavelet was used to correct eye blinks artifacts (Castellanos & Makarov, 2006). The last method applies a wavelet thresholding to the demixed independent components as an intermediate step, which enables recovering the neural activity present in artefactual components. In this case, we use a threshold of 0,1, which represents the probability that the component was neuronal. This probability was calculated by the Multiple Artifact Rejection Algorithm (Winkler, Haufe, & Tangermann, 2011).

Data were resampled to 200 Hz and used to calculate 8 regions of interest (ROI's) as the average of channels in each ROI (Figure 2). These regions correspond to frontal, parietal and occipital areas of each hemisphere.
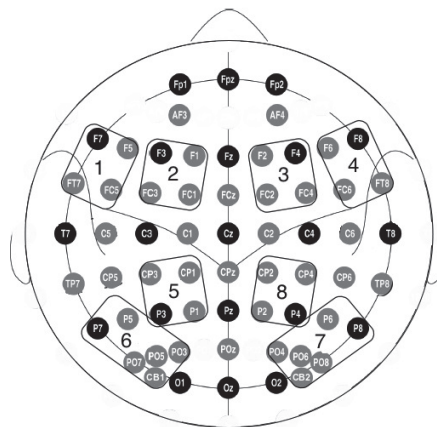

Figure 2. Electrode distribution according to 10-10 system used in the recording of the EEG data and ROI's calculated (Oostenveld & Praamstra, 2001).

Direct Directed Transfer Function and Graph construction

For each subject, a sliding-window Adaptive Multivariate Autoregressive (AMVAR) model was fitted to the 1 s time series, where the time series correspond to the signal in each ROI. The dDTF was estimated using the Source Information Flow Toolbox (Delorme *et al.*, 2011). The length of the sliding-window was 250 ms with a window step of 10 ms. The parameters used to fit the model are shown in Table 2.

Table 2. AMVAR model parameters

Parameter	Value
Model Order	9,24 ± 1,15
Window step	0,01 s
Window length	0,25 s
Consistency	(74,48 ± 10,58) %
Stability	100 %

Mean ± standard deviation.

In each sliding-window the dDTF is calculated as follows:

$$d\,_{ij}^{2}(f) = n\,_{ij}^{2}(f)k\,_{ij}^{2}(f) \tag{1}$$

$$n_{ij}^{2} = \frac{\left|H_{ij}(f)\right|^{2}}{\sum_{f}\sum_{m=1}^{k}\left|H_{ij}(f)^{2}\right|} \tag{2}$$

$$k_{ij}(f) = \frac{\widehat{S}_{ij}(f)}{\sqrt{\widehat{S}_{ii}(f)\widehat{S}_{jj}(f)}} \tag{3}$$

$$\widehat{S}_{ij}(f) = S(f)^{-1} \tag{4}$$

Where f is the frequency, $n_{ij}^{2}(f)$ is the full frequency DTF (ffDTF) (Equation (2)), $k_{ij}^{2}(f)$ is the partial coherence (Equation (3)), H_{ij} is the system transfer matrix obtained after the z-transform of the AMVAR model, and $S(f)$ is the spectral density matrix. Indices i, j refer to signals in ROIs i and j.

The dDTF was analyzed in alpha1 frequency band (8–10 Hz), which is related to memory processes (Klimesch, Freunberger, & Sauseng, 2010), for time widows of 100 ms along each 1 s epoch. At each interval, an 8×8 matrix was obtained where each entry (i,j) correspond to the connectivity between the ROI-i and the ROI-j.

The new matrices were normalized according to the recommendations given by Ahnert *et al.* (Ahnert, Garlaschelli, Fink, & Caldarelli, 2007), to avoid the definition of a threshold for the comparison between groups. Three graphs measures were obtained: total strength, in-strength, and out-strength (Rubinov & Sporns, 2010). Total strength is the sum of weights of links connected to the node:

$$k_{i}^{p} = \sum_{j \in N} P_{ij} + \sum_{j \in N} P_{ji} \tag{5}$$

Where k_{i}^{p} is the node strength, N is the set of all nodes in the network and P_{ji} are the connection weights between node i and j. In-strength is the sum of inward link weights and out-strength is the sum of outward link weights.

Statistical analysis

Given that the main motivation of this study is to identify a biomarker in EEG connectivity features that allows the tracking of the neurodegenerative process, the first step was a correlation analysis of each connectivity measurement with age and MMSE in the carriers (ACr and MCI) and non-carriers (Control1 and Control2). This analysis was conducted for each ROI separately trying to find regions where the connectivity was related to the age or the neuropsychological scale. The performance of the measurements as diagnostic variables were quantified by calculating the area under the receiver operating characteristic curves (AUROC). In view of differences in age in these groups (p = 0,05), data were corrected for this variable using linear regression.

Results

There were no differences in gender, education or neuropsychological examination between ACr and Control1 (Table 1) as were expected, because of the asymptomatic condition of this groups. We found differences in MMSE examination between MCI patients and Control2 subjects. Regarding behavioral data, there were no significant differences between ACr and Control1 for reaction time (p > 0,1). Comparing MCI and Control2 groups, MCI group has a longer reaction time (p < 0,05) and a lower recognition score after the encoding stage (p < 0,05).

No significant correlations for measures of in-strength and total strength were found in any ROI. Only a significant correlation for out-strength was found. Table 3 shows the correlation analysis results between out-strength connectivity and age, and out-strength connectivity and MMSE. This measure had significant correlation only for the carriers group in ROI7. In the non-carriers group there were no significant associations.

Figure 3 shows plots of out-strength mean in ROI7 for the groups across the ten time windows defined in the methodology. It shows a variation of the measurement along the time for each group and a difference in values

among the groups. Since the data does not meet the assumptions for analysis of variance, we chose to use measures of effect size to calculate the magnitude of the difference between the groups, using the Hedges' g (standardized mean difference) (Hentschke & Stüttgen, 2011) in each time interval. The results showed a higher out-strength for ACr group compared with Control1 on 600 ms (Hedges = 0,698, CI = 0,015 – 1,595), and 800 ms (Hedges = 0,742, CI = 0,097 – 1,402). Also, decreased out-strength for MCI group compared to Control2 was found on 600 ms (Hedges = −0,872, CI = −1,640 – (−0,209).
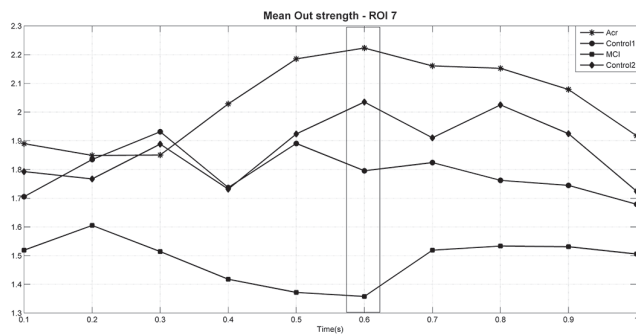
Figure 3. Out-strength mean for each group in ROI 7. How the connectivity is estimated in time windows of 100 – ms, the plot shows how the connectivity changes for each time window across the 1 – s epoch. The rectangle refers to the time interval in which out-strength presented statistically significant differences. ACr: asymptomatic mutation carriers; MCI: Mild Cognitive Impairment; Control1 and Control2: non-carriers.

Table 4 describes the AUROC analysis for the intervals of out-strength in ROI 7. The table includes a threshold for each variable where both sensitivity and specificity are higher (best cut-off). The best diagnosis interval was (500 – 600) ms comparing both ACr and Control1, and MCI and Control2 groups, which presented the highest AUROC values.

Table 3. Results of Correlation analysis for out-strength connectivity in carriers and non-carriers.

ROI	Carriers				Noncarriers			
	Age		MMSE		Age		MMSE	
	CC	P-value	CC	P-value	CC	P-value	CC	P-value
1	−0,29	0,14	0,011	0,95	−0,051	0,8	−0,3	0,13
2	−0,027	0,89	−0,12	0,54	−0,23	0,25	−0,05	0,8
3	−0,21	0,29	0,36	0,066	−0,005	0,8	−0,039	0,85
4	−0,42	0,031	0,38	0,05	−0,093	0,64	−0,18	0,37
5	−0,25	0,21	0,14	0,49	0,20	0,31	0,26	0,18
6	−0,24	0,22	0,072	0,72	0,19	0,34	−0,063	0,76
7	**−0,54**	**0,0036**	**0,37**	**0,058**	−0,016	0,94	−0,059	0,77
8	−0,11	0,58	−0,054	0,79	0,11	0,59	0,26	0,19

ROI: region of interest; CC: correlation coefficient.

Discussion

In this work we studied the relationship between connectivity measurements and cognitive impairment and its performance as a diagnostic variable. We found that out-strength, a measure related to effective connectivity, in the right occipito-parietal region (ROI 7) is related to age, and hence to neurodegenerative process, in individuals carrying the PSEN1 E280A mutation. The fact that this relationship is only present in the aforementioned group of individuals indicates that the measurement could be related to the neurodegenerative process. By analyzing the temporal behavior of measurements in ROI 7, we found that in the 500-600 ms period it is possible to differentiate between ACr and Control1 groups with 67 % sensitivity and 80 % specificity, and between the MCI and Control2 groups with 83 % sensitivity and 67 % specificity.

Table 4. Individual AUROCs. Table lists the area under the ROC curves and confidence intervals for the ten time windows where differences between ACr patients and Control1 subjects, and MCI patients and Control2 subjects were found. For each ROC curve, we select the best cut-off point (threshold) for out-strength and calculated the respective sensitivity and specificity values.

Epoch (ms)	AUROC	CI	Threshold	Sensitivity	Specificity	PPV	NPV
ACr vs Control1							
0–100	0,57	0,35-0,79	0,37	0,47	0,87	0,78	0,62
100–200	0,53	0,31-0,75	-0,14	0,67	0,53	0,59	0,62
200–300	0,52	0,29-0,74	-0,03	0,67	0,53	0,59	0,62
300–400	0,72	0,52-0,91	-0,35	0,93	0,53	0,67	0,89
400–500	0,68	0,47-0,88	-0,17	0,80	0,53	0,63	0,73
500–600	0,71	0,51-0,90	0,13	0,67	0,80	0,77	0,71
600–700	0,64	0,43-0,85	0,14	0,53	0,80	0,73	0,63
700–800	0,66	0,45-0,86	0,30	0,40	0,93	0,86	0,61
800–900	0,70	0,49-0,91	0,18	0,60	0,93	0,90	0,70
900-1000	0,64	0,44-0,85	-0,40	0,93	0,40	0,61	0,86
MCI vs Control2							
0–100	0,62	0,37-0,86	-0,27	0,58	0,75	0,70	0,64
100–200	0,48	0,23-0,73	0,12	0,42	0,75	0,63	0,56
200–300	0,44	0,19-0,70	0,16	0,50	0,75	0,67	0,60
300–400	0,44	0,19-0,68	0,02	0,50	0,58	0,55	0,54
400–500	0,66	0,43-0,89	-0,15	0,58	0,75	0,70	0,64
500–600	0,76	0,56-0,96	0,07	0,83	0,67	0,71	0,80
600–700	0,59	0,35-0,83	0,16	0,83	0,42	0,59	0,71
700–800	0,67	0,44-0,90	-0,22	0,58	0,75	0,70	0,64
800–900	0,61	0,37-0,85	-0,36	0,42	0,92	0,83	0,61
900-1000	0,56	0,31-0,80	0,03	0,67	0,58	0,62	0,64

AUROC: area under the ROC curve; CI: confidence interval; PPV: positive predictive value; NPV: negative predictive value.

Previous studies of PSEN1 E280A mutation using EEG have shown an alteration in brain function in presymptomatic disease cases. By estimating intracranial sources of evoked potentials (ERPs), lower N400 amplitudes were found in symptomatic carriers compared with presymptomatic carriers and non-carriers. In addition, the topography differed in the mutation carrier group with respect to the non-carriers (Bobes *et al*., 2010). Other ERPs study, which examines dynamic brain function in young presymptomatic carriers in a visual recognition process, found that despite an identical behavioral performance, the carriers showed lower positivity in frontal regions and increased positivity in occipital regions compared with control subjects. These differences were more pronounced during the (200-300) ms period. Discriminant analysis at this time interval showed promising sensitivity (72,7 %) and specificity (81,8 %) for predicting the presence of AD (Y T Quiroz *et al*., 2011).

Brain activity in the occipital region has been associated with visual perceptual processing (Cronin-Golomb, Gilmore, Neargarder, Morrison, & Laudate, 2007). AD is thought to cause a functional decline associated with posterior cortical dysfunction, and a variety of visual disorders including impairments of contrast sensitivity, motion perception and navigation. In fact, navigation has been associated with memory problems observed in AD (Ally, McKeever, Waring, & Budson, 2009). The pattern of posterior connectivity observed in the ACr group may reflect an early AD-related synaptic dysfunction or a neural compensation process that requires that carriers use posterior regions more in recognition memory in order to perform equally well as the controls. A positron emission tomography study by Fleisher *et al*, (2015) found that, compared with non-carriers, cognitively unimpaired PSEN1 E280A mutation carriers have significantly lower precuneus cerebral metabolic rates for glucose. The reduction in brain metabolism and atrophy may be reflected by an increment in functional connectivity. Evidences about connectivity changes that might be related to increased neuronal activity, as a possible compensatory mechanisms, were found using fMRI (Yakeel T Quiroz *et al.,* 2010), and EEG (Ochoa *et al*., 2015).

Here we found that connectivity in MCI carrier patients decreases compared with the other groups. The MCI group presents an initial state of the neurodegenerative process of dementia with a loss of cognitive functions (MMSE significantly lower compared with Control2). Connectivity studies with EEG have shown a reduced synchronization in sporadic AD and MCI patients for delta and beta bands, and a progressive decrease in alpha1 synchronization through the disease states (Babiloni *et al.,* 2006). Our results suggest that the decrease in connectivity in MCI carriers could occur by this loss of synchronization during the progression of the disease, and that in this state, the dynamics of EEG are similar in PSEN1 E280A mutation carriers and sporadic AD.

Overall, our results are consistent with connectivity and ERP studies and show that EEG connectivity measurements could be used as markers for the detection and monitoring of AD in PSEN1 E280A mutation carriers. Compared to ERPs analysis, which are mainly based on averages of the signal, the study of graph functional connectivity is an alternative for a more systematic analysis of the brain, where a measure may represent important information about both local and global organization of brain functioning.

Conclusions

The order and magnitude of pathological processes in AD are not well understood, partly because of the lack of an early diagnostic tool that enables the study of the evolution of the disease. Autosomal dominant Alzheimer's disease has a predictable age at onset and provides an opportunity to determine the sequence and magnitude of pathological changes that culminate in symptomatic disease. Our results show that effective connectivity is related to age in the carrier group and therefore may be related to neurodegenerative processes. This provides an opportunity to test new biomarkers in AD. The next step is to study the evolution of the proposed effective connectivity in a longitudinal study.

Acknowledgment

References

Aguirre-Acevedo, D. C., Gómez, R. D., Moreno, S., Henao-Arboleda, E., Motta, M., Muñoz, C., … Lopera, F. (2007). Validez y fiabilidad de la batería neuropsicológica CERAD-Col. *Revista de Neurolgía*, *45*(11), 655–660.

Ahnert, S. E., Garlaschelli, D., Fink, T. M. A., & Caldarelli, G. (2007). Ensemble approach to the analysis of weighted networks. *Physical Review. E, Statistical, Nonlinear, and Soft Matter Physics*, *76*(1 Pt 2), 16101.

Ally, B. A., McKeever, J. D., Waring, J. D., & Budson, A. E. (2009). Preserved frontal memorial processing for pictures in patients with mild cognitive impairment. *Neuropsychologia*, *47*(10), 2044–2055.
DOI: 10.1016/j.neuropsychologia.2009.03.015

Ardila, A., Lopera, F., Rosselli, M., Moreno, S., Madrigal, L., Arango-Lasprilla, J. C., … Kosik, K. S. (2000). Neuropsychological profile of a large kindred with familial Alzheimer's disease caused by the E280A single presenilin-1 mutation. *Archives of Clinical Neuropsychology: The Official Journal of the National Academy of Neuropsychologists*, *15*(6), 515–528.

Babiloni, C., Ferri, R., Binetti, G., Cassarino, A., Dal Forno, G., Ercolani, M., … Rossini, P. M. (2006). Fronto-parietal coupling of brain rhythms in mild cognitive impairment: a multicentric EEG study. *Brain Research Bulletin*, *69*(1), 63–73. DOI: 10.1016/j.brainresbull.2005.10.013

Bertram, L., & Tanzi, R. E. (2011). Genetics of Alzheimer's Disease. *Neurodegeneration: The Molecular Pathology of Dementia and Movement Disorders: Second Edition*. DOI: 10.1002/9781444341256.ch9

Bobes, M. a, García, Y. F., Lopera, F., Quiroz, Y. T., Galán, L., Vega, M., … Valdes-Sosa, P. (2010). ERP generator anomalies in presymptomatic carriers of the Alzheimer's disease E280A PS-1 mutation. *Human Brain Mapping*, *31*(2), 247–65. DOI: 10.1002/hbm.20861

Bullmore, E. T., & Bassett, D. S. (2011). Brain graphs: graphical models of the human brain connectome. *Annual Review of Clinical Psychology*, *7*, 113–40. DOI: 10.1146/annurev-clinpsy-040510-143934

Castellanos, N. P., & Makarov, V. A. (2006). Recovering EEG brain signals: Artifact suppression with wavelet enhanced independent component analysis. *Journal of Neuroscience Methods*, *158*, 300–312. DOI: 10.1016/j.jneumeth.2006.05.033

Cronin-Golomb, A., Gilmore, G. C., Neargarder, S., Morrison, S. R., & Laudate, T. M. (2007). Enhanced stimulus strength improves visual cognition in aging and Alzheimer's disease. *Cortex; a Journal Devoted to the Study of the Nervous System and Behavior*, *43*(7), 952–966.

Delorme, A., & Makeig, S. (2004). EEGLAB: An open source toolbox for analysis of single-trial EEG dynamics including independent component analysis. *Journal of Neuroscience Methods*, *134*, 9–21. DOI: 10.1016/j.jneumeth.2003.10.009

Delorme, A., Mullen, T., Kothe, C., Akalin Acar, Z., Bigdely-Shamlo, N., Vankov, A., & Makeig, S. (2011). EEGLAB, SIFT, NFT, BCILAB, and ERICA: New tools for advanced EEG processing. *Computational Intelligence and Neuroscience*, *2011*. DOI: 10.1155/2011/130714

Delorme, A., Sejnowski, T. J., & Makeig, S. (2007). Enhanced detection of artifacts in EEG data using higher-order statistics and independent component analysis. *Neuroimaging*, *34*(4), 1443–1449. DOI: 10.1016/j.neuroimage.2006.11.004.Enhanced

Duque-Grajales, J. E., Tobón, C., Aponte-Restrepo, C. P., Ochoa-Gomez, J. F., Muñoz-Zapata, C., Hernández-Valdivieso, A. M., … Lopera, F. (2014). Quantitative EEG analysis disease during resting and memory task in carriers and non-carriers of PS-1 E280A mutation of familial Alzheimer´s. *Revista CES Medicina*, *28*(2), 165–176.

Fleisher, A. S., Chen, K., Quiroz, Y. T., Jakimovich, L. J., Gutierrez Gomez, M., Langois, C. M., … Reiman, E. M. (2015). Associations Between Biomarkers and Age in the Presenilin 1 E280A Autosomal Dominant Alzheimer Disease Kindred: A Cross-sectional Study. *JAMA Neurology*, *72*(3), 316–324. DOI: 10.1001/jamaneurol.2014.3314

Hafkemeijer, A., van der Grond, J., & Rombouts, S. A. R. B. (2012). Imaging the default mode network in aging and dementia. *Biochimica et Biophysica Acta (BBA) - Molecular Basis of Disease*, *1822*(3), 431–441. DOI: 10.1016/j.bbadis.2011.07.008

He, Y., Chen, Z., Gong, G., & Evans, A. (2009). Neuronal networks in Alzheimer's disease. *The Neuroscientist: A Review Journal Bringing Neurobiology, Neurology and Psychiatry*, *15*(4), 333–350. DOI:10.1177/1073858409334423

Hentschke, H., & Stüttgen, M. C. (2011). Computation of measures of effect size for neuroscience data sets. *European Journal of Neuroscience*, *34*(July), 1887–1894. DOI: 10.1111/j.1460-9568.2011.07902.x

Hsiao, F.-J., Wang, Y.-J., Yan, S.-H., Chen, W.-T., & Lin, Y.-Y. (2013). Altered oscillation and synchronization of default-mode network activity in mild Alzheimer's disease compared to mild cognitive impairment: an electrophysiological study. *PloS One*, *8*(7), e68792. DOI: 10.1371/journal.pone.0068792

Klimesch, W., Freunberger, R., & Sauseng, P. (2010). Oscillatory mechanisms of process binding in memory. *Neuroscience and Biobehavioral Reviews*, *34*(7), 1002–1014. DOI: 10.1016/j.neubiorev.2009.10.004

Langbaum, J. B., Fleisher, A. S., Chen, K., Ayutyanont, N., Lopera, F., Quiroz, Y. T., … Reiman, E. M. (2013). Ushering in the study and treatment of preclinical Alzheimer disease. *Nature Reviews. Neurology*, *9*(7), 371–81. DOI: 10.1038/nrneurol.2013.107

Lopera, F., Ardilla, A., Martínez, A., Madrigal, L., Arango-Viana, J. C., Lemere, C. A., … Kosik, K. S. (1997). Clinical features of early-onset Alzheimer disease in a large kindred with an E280A presenilin-1 mutation. *Journal of the American Medical Association*, *277*(10), 793–799.

Micanovic, C., & Pal, S. (2014). The diagnostic utility of EEG in early-onset dementia: a systematic review of the literature with narrative analysis. *Journal of Neural Transmission (Vienna, Austria: 1996)*, *121*(1), 59–69. DOI: 10.1007/s00702-013-1070-5

Minati, L., Edginton, T., Bruzzone, M. G., & Giaccone, G. (2009). Current concepts in Alzheimer's disease: a multidisciplinary review. *American Journal of Alzheimer's Disease and Other Dementias*, *24*(2), 95–121. DOI: 10.1177/1533317508328602

Ochoa, J., Sánchez, F., Tobón, C., Duque, J., Quiroz, Y., Lopera, F., & Hernandez, M. (2015). Effective Connectivity Changes in Presymptomatic Alzheimer's Disease with E280A Presenilin-1 Mutation Gene. In A. Braidot & A. Hadad (Eds.), *VI Latin American Congress on Biomedical Engineering CLAIB 2014, Paraná, Argentina 29, 30 & 31 October 2014 SE - 130* (Vol. 49, pp. 508–511). Springer International Publishing. DOI:10.1007/978-3-319-13117-7_130

Oostenveld, R., & Praamstra, P. (2001). The five percent electrode system for high-resolution EEG and ERP measurements. *Clinical Neurophysiology: Official Journal of the International Federation of Clinical Neurophysiology*, *112*(4), 713–719.

Ouchi, Y., & Kikuchi, M. (2012). A review of the default mode network in aging and dementia based on molecular imaging. *Reviews in the Neurosciences*, *23*(3), 263–268. DOI: 10.1515/revneuro-2012-0029

Pievani, M., de Haan, W., Wu, T., Seeley, W. W., & Frisoni, G. B. (2011). Functional network disruption in the degenerative dementias. *Lancet Neurology*, *10*(9), 829–43. DOI: 10.1016/S1474-4422(11)70158-2

Quiroz, Y. T., Ally, B. a, Celone, K., McKeever, J., Ruiz-Rizzo, a L., Lopera, F., … Budson, a E. (2011). Event-related potential markers of brain changes in preclinical familial Alzheimer disease. *Neurology*, *77*(5), 469–75. DOI: 10.1212/WNL.0b013e318227b1b0

Quiroz, Y. T., Budson, A. E., Celone, K., Ruiz, A., Newmark, R., Castrillon, G., … Stern, C. E. (2010). Hippocampal

hyperactivation in presymptomatic familial Alzheimer's disease. *Annals of Neurology*, *68*(6), 865–875. DOI: 10.1002/ana.22105

Quiroz, Y. T., Stern, C. E., Reiman, E. M., Brickhouse, M., Ruiz, A., Sperling, R. A., … Dickerson, B. C. (2013). Cortical atrophy in presymptomatic Alzheimer's disease presenilin 1 mutation carriers. *Journal of Neurology, Neurosurgery, and Psychiatry*, *84*(5), 556–561. DOI: 10.1136/jnnp-2012-303299

Rodriguez, R., Lopera, F., Alvarez, A., Fernandez, Y., Galan, L., Quiroz, Y., & Bobes, M. A. (2014). Spectral Analysis of EEG in Familial Alzheimer's Disease with E280A Presenilin-1 Mutation Gene. *International Journal of Alzheimer's Disease*, *201WW4*, 180741. DOI: 10.1155/2014/180741

Rubinov, M., & Sporns, O. (2010). Complex network measures of brain connectivity: uses and interpretations. *NeuroImage*, *52*(3), 1059–69.

DOI: 10.1016/j.neuroimage.2009.10.003

Sanz-Arigita, E. J., Schoonheim, M. M., Damoiseaux, J. S., Rombouts, S. A. R. B., Maris, E., Barkhof, F., … Stam, C. J. (2010). Loss of "small-world" networks in Alzheimer's disease: graph analysis of FMRI resting-state functional connectivity. *PloS One*, *5*(11), e13788. DOI: 10.1371/journal.pone.0013788

Sperling, R., Mormino, E., & Johnson, K. (2014). The Evolution of Preclinical Alzheimer ' s Disease: Implications for Prevention Trials. *Neuron*, *84*(3), 608–622. DOI: 10.1016/j.neuron.2014.10.038

Stam, C. J., de Haan, W., Daffertshofer, A., Jones, B. F., Manshanden, I., van Cappellen van Walsum, A. M., … Scheltens, P. (2009). Graph theoretical analysis of magnetoencephalographic functional connectivity in Alzheimer's disease. *Brain: A Journal of Neurology*, *132*(Pt 1), 213–24. DOI: 10.1093/brain/awn262

Supekar, K., Menon, V., Rubin, D., Musen, M., & Greicius, M. D. (2008). Network analysis of intrinsic functional brain connectivity in Alzheimer's disease. *PLoS Computational Biology*, *4*(6), e1000100. DOI: 10.1371/journal.pcbi.1000100

Tobon, C., Duque, J. E., Ochoa, J. F., Hernandez, M., Quiroz, Y. T., & Lopera, F. (2015). CHANGES IN BRAIN NETWORK MEASURES IN PRE-SYMPTOMATIC ALZHEIMER'S DISEASE WITH E280A PRESENILIN-1 MUTATION GENE. *Alzheimer's & Dementia: The Journal of the Alzheimer's Association*, *10*(4), P885–P886. DOI: 10.1016/j.jalz.2014.07.047

Winkler, I., Haufe, S., & Tangermann, M. (2011). Automatic Classification of Artifactual ICA-Components for Artifact Removal in EEG Signals. *Behavioral and Brain Functions*, *7*(1), 30. DOI: 10.1186/1744-9081-7-30

Xie, T., & He, Y. (2011). Mapping the Alzheimer's brain with connectomics. *Frontiers in Psychiatry*, *2*(January), 77. DOI: 10.3389/fpsyt.2011.00077